Clinical Plasma Medicine 14 (2019) 100083

Contents lists available at ScienceDirect

Clinical Plasma Medicine

journal homepage: www.elsevier.com/locate/cpme

Original research article

Cold physical plasma-induced oxidation of cysteine yields reactive sulfur species (RSS)

Giuliana Bruno[a], Thea Heusler[a], Jan-Wilm Lackmann[a], Thomas von Woedtke[b,c], Klaus-Dieter Weltmann[b], Kristian Wende[a,*]

[a] ZIK plasmatis, Leibniz Institute for Plasma Science and Technology (INP Greifswald), Felix-Hausdorff-Straße 2, 17489 Greifswald, Germany
[b] Leibniz Institute for Plasma Science and Technology (INP Greifswald), Felix-Hausdorff-Straße 2, 17489 Greifswald, Germany
[c] Greifswald University Medicine, Fleischmannstraße 8, 17475 Greifswald, Germany

ARTICLE INFO

Keywords:
Redox signaling
Plasma liquid chemistry
Reactive sulfur species
Cold physical plasma
CAP

ABSTRACT

Purpose: Studying plasma liquid chemistry can reveal insights into their biomedical effects, i.e. to understand the direct and indirect processes triggered by the treatment in a model or clinical application. Due to the reactivity of the sulfur atom, thiols are potential targets for plasma- derived reactive species. Being crucial for protein function and redox signaling pathways, their controllable modification would allow expanding the application range. Additionally, models to control and standardize CAP sources are desired tools for plasma source design.
Methods: Cysteine, a ubiquitous amino acid, was used as a tracer compound to scavenge the reactive species produced by an argon plasma jet (kINPen). The resulting product pattern was identified via high-resolution mass spectrometry. The Ellman´s assay was used to screen CAP derived thiol consumption, and long-lived species deposition (hydrogen peroxide, nitrite, nitrate) was monitored in relation to the presence of cysteine.
Results: The intensity of cysteine oxidation increased with treatment time and availability of oxygen in the feed gas. A range of products from cysteine was identified, in part indicative for certain treatment conditions. Several non-stable products occur transiently during the plasma treatment. Bioactive reactive sulfur species (RSS) have been found for mild treatment conditions, such as cysteine sulfoxides and cysteine-*S*-sulfonate. Considering the number of cysteine molecules in the boundary layer and the achieved oxidation state, short-lived species dominate in cysteine conversion. In addition, a boundary layer depletion of the tracer was observed.
Conclusion: Translating these data into the in-vivo application, strong direct oxidation of protein thiol groups with subsequent changes in protein biochemistry must be considered. Plasma-derived RSS may in part contribute to the observed biomedical effects of CAP. Care must be taken to control the discharge parameter tightly as chemical dynamics at or in the liquid are subject to change easily.

1. Introduction

Plasma medicine has emerged as a therapeutic alternative in the area of cancer treatment and skin related acute and chronic diseases, such as acute or infected chronic wounds [1–4]. The enabling technology is cold atmospheric plasma (CAP) that can be generated by various sources, with plasma jets (APPJs) and dielectric barrier discharges (DBDs) being the most prevalent options for biomedical applications [3,5,6]. All CAPs are characterized by the action of a complex mixture of chemical entities, like electrons, ions, neutrals, and radical species as well as radiation and electric fields. This highly dynamic system so far successfully prevented the full discovery of all relevant entities in clinical application and in vitro research, especially when focusing the liquid compartment like a tissue or cell [7]. In contrast, the gas phase composition of some CAPs is considerably well characterized, e.g. for kINPen [8–10], RF plasma jet [11–13], and the COST jet [14–16]. The reactive species considered most interesting in the biomedical field are those deposited in the liquid phase of a treated tissue or model cell system. Their origin and biochemical potential are under study, considering the large variety of species composition due to the different plasma sources and applied parameters (e.g. flow rate, energy input, working gas composition) and treatment conditions (e.g. distance to the target, duration). Even less understood is the role of the gas-liquid interphase and the subsequent transport of species into the liquid bulk. The chemical composition of the treated system further modulates the formation, propagation, and stability of primary and secondary/

* Corresponding author.
E-mail address: kristian.wende@inp-greifswald.de (K. Wende).

https://doi.org/10.1016/j.cpme.2019.100083
Received 28 May 2018; Received in revised form 14 February 2019; Accepted 8 March 2019

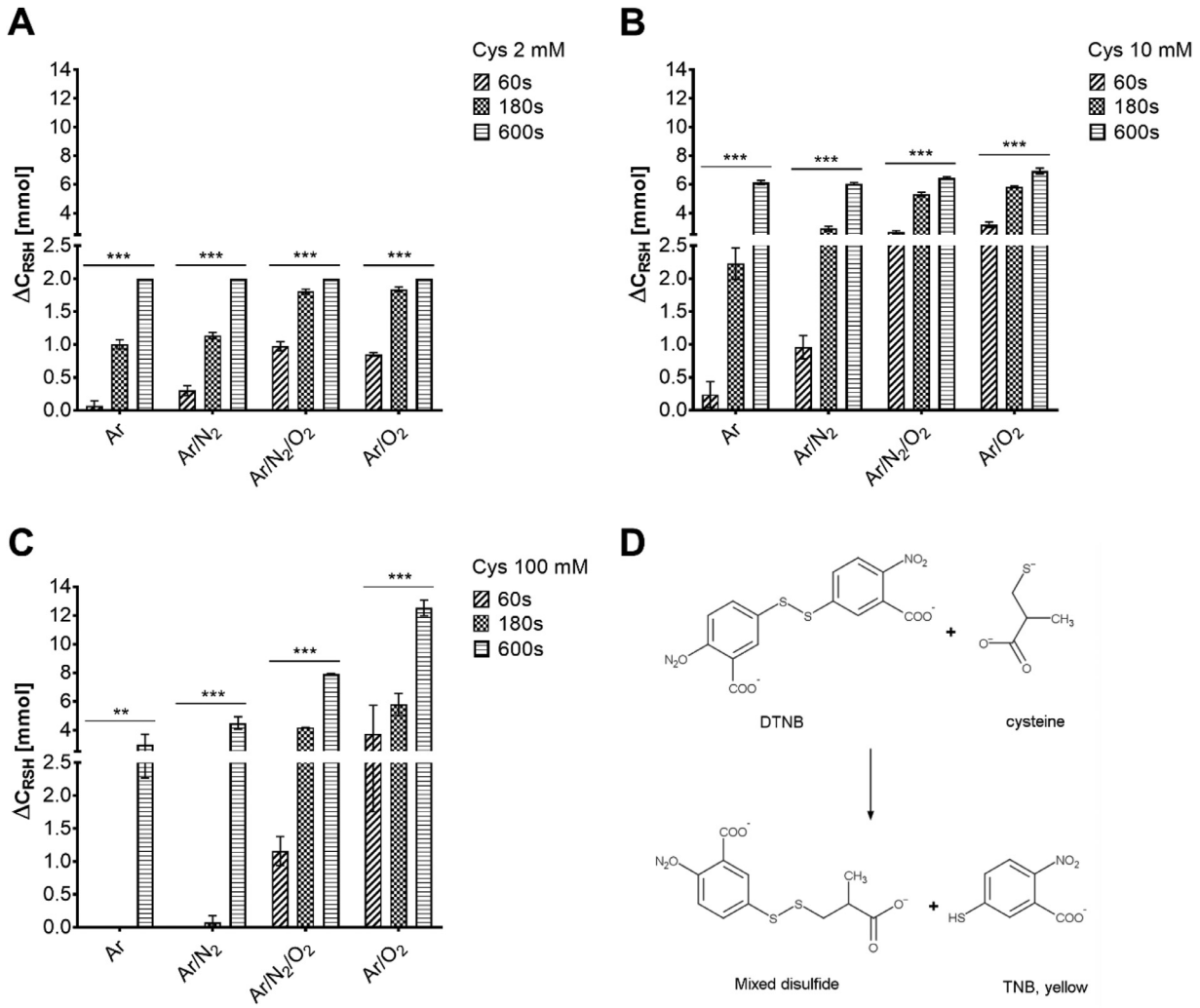

Fig. 1. Cysteine oxidation by varying the used feed gas, the duration of the treatment and cysteine concentration in 2 mM (A), 10 mM (B) and 100 mM (C), reaction scheme Ellman´s assay (D) kINPen09, 3 slm Ar + 1% molecular gas admix.

tertiary species, and finally the efficacy of the plasma treatment.

In case of the argon-based kINPen, central primary species in the gas phase are metastable argon (Ar*) and argon excimers (Ar_2*). Secondary gas phase species are formed by interaction of primary species and feed gas admixtures (e.g. O_2, N_2) or ambient species, creating species as hydroxyl radicals (•OH), atomic oxygen (•O), singlet oxygen ($^1O_2$), ozone (O_3), atomic nitrogen (•N), and nitric oxides (N_xO_y) [17]. Secondary species can also be produced in the liquid by the impact of plasma-generated species, radiation, electrons; in this case, species as hydroxyl radicals (•OH), superoxide radicals ($•O_2^-$), nitrous (HNO_2), nitric acid (HNO_3), or peroxynitrite ($ONOO^-$) can be formed [18,19]. By interaction with ions or molecules present in the treated target, additional species like hypochlorite (OCl^-) can evolve [20]. Most of these species are hard to quantify with reasonable specificity, e.g. ozone, singlet oxygen, or hydroxyl radicals. Using electron paramagnetic resonance (EPR) radical species can be detected in CAP treated liquids, but quantitative statements are debatable [18,21,22]. In contrast, for the "stable" species H_2O_2, nitrite, and nitrate various quantitative chemical assays exist, which subsequently led to the impression that these are of predominant biomedical relevance [9,23], e.g. H_2O_2 [24], or nitric oxide [25].

Taking the recent publications on short-lived species into account it must be assumed that also they can reach the biological target and in part control or at least modulate the functional outcome of CAP treatment. Given the poor selectivity of existing assay methods, chemically modifiable tracer molecules pose an alternative way to study plasma liquid chemistry. Under controlled conditions, cysteine is a suitable sensitive and reactive molecule. Zhou et al. identified cysteine sulfonic acid beside cystine as major products after CAP treatment [26]. Especially its thiol moiety can be distinctively oxidized by CAP derived species, making cysteine a potential model for standardization efforts using the product pattern evolving by the CAP treatment as a fingerprint [27,28]. Furthermore, the amino acid is a ubiquitous and essential component of proteins and important partner in many redox-signaling processes, able to act both as an electron acceptor and donor [29]. Therefore, cysteine is present in body fluids and cell culture media, e.g. Dulbecco's Modified Eagle Medium (DMEM). With that, detailed knowledge of CAP derived species interaction with cysteine and related compounds is desirable as this may both prohibit and retard their impact in biological systems [30,31]. Subsequently, CAP derived cysteine derivatives, especially reactive sulfur species (RSS), could in turn influence the cellular redox balance [29, 32–34].

Here, an in-depth study of the CAP treatment derived cysteine product pattern beyond cystine and cysteine sulfonic acid is presented with the aim to foster plasma treatment standardization, to understand reactive species trajectories, and to estimate effects on thiols in biomolecules in vitro and in vivo.

Table 1
Number of cysteine molecules present and oxidized during treatment (calculated, measured or assumed on models) and number of one electron equivalent species hitting the target during kINPen treatment of 24-well plate, 750 µl volume of 2/10/100 mM cysteine solution.

Cysteine solution	No of cysteine molecules				Number of one-electron acceptor equivalents			
	Per cm^3	In vessel (0.75 cm^3)	In boundary surface (30 mm^3) model [38] $/s^{-1}$	In boundary surface (0.36 mm^3) measure [39] $/s^{-1}$	Oxidized cysteine molecules Ar/O_2, 60 s (Ellman's) $/s^{-1}$	Cysteine > > cystine $/s^{-1}$	Cysteine > > cysteine sulfonic acid $/s^{-1}$	Hitting target (O, [a]O_2, O_3, OH)[a] $/s^{-1}$
2 mM	1.20×10^{18}*	9.00×10^{17}*	3.60×10^{16}#	6.32×10^{14}#	5.62×10^{15}+	5.62×10^{15}*	2.81×10^{16}*	6.09×10^{16}#
10 mM	6.00×10^{18}*	4.50×10^{18}*	1.80×10^{17}#	2.16×10^{15}#	2.55×10^{16}+	2.55×10^{16}*	1.27×10^{17}*	6.09×10^{16}#
100 mM	6.00×10^{19}*	4.50×10^{19}*	1.80×10^{18}#	2.16×10^{16}#	3.00×10^{16}+	3.00×10^{16}*	1.50×10^{17}*	6.09×10^{16}#

* Calculated.
\# Assumed.
\+ Measured.
[a] One-electron acceptor equivalents used for calculation: hydroxyl radical = 1, atomic O = 2, singlet oxygen = 4, ozone = 6; species densities according to [17].

2. Materials and methods

2.1. Plasma source

The kINPen09 (neoplas GmbH, Germany), an atmospheric pressure plasma jet using argon as main feed gas was used in this study. It is driven by an alternating current at ≈ 1 MHz / 2–6 kV, with 1.1 W power deposition in the discharge. The central high-voltage electrode has a diameter of 1.6 mm and is surrounded by a ceramic capillary. If desired, the plasma effluent was shielded from ambient air by a controllable gas curtain [8].

2.2. Sample preparation and plasma treatments

Cysteine solutions with various concentrations (300 µM, 2 mM, 10 mM, and 100 mM) were freshly prepared from cysteine (L-Cysteine, Sigma-Aldrich Co. LLC., St. Louis, USA) using double-distilled water (ddH_2O) (MilliQ, Milli-Q® Merck KGaA, Darmstadt, Germany), or 5 mM phosphate buffered saline pH 7.4. 750 µL of each solution was treated directly in 24 well-plate for 45, 60, 180, 300 or 600 s, with a fixed distance jet's nozzle-liquid surface of 9 mm. A flow rate of 3 standard liters per minute (slm) of dry argon (argon N50, Air Liquide, Paris, France) was used as feed gas and for some experiments, 1% of nitrogen (nitrogen N50, Air Liquide, Paris, France), oxygen (oxygen N48, Air Liquide, Paris, France), or a 1:1 mixture of both was added. Treatments were made either with or without curtain gas (5 slm nitrogen or oxygen) around the effluent to reduce the impact of the ambient atmosphere.

2.3. Colorimetric assays

Ellman´s reagent, or 5,5′-dithiobis-(2-nitrobenzoic) acid (DTNB, Sigma-Aldrich Co. LLC., St. Louis, USA), was used for the quantification of residual non-oxidized thiol groups in the treated cysteine solutions. The reaction solution consisted of 1 mM DTNB, 1 mM EDTA, 10 mM PO_4^{3-} and 144 mM NaCl. The DTNB is a disulfide consisting of two TNB molecules (2-nitro-5-thiobenzoate). It is reacting with the free thiols of cysteine by releasing a TNB molecule and forming a mixed disulfide between cysteine and the other TNB molecule. The absorbance of these is then detected at 412 nm (Tecan Infinite M200 Pro, Tecan Group Ltd., Männedorf, Switzerland). Hydrogen peroxide (H_2O_2) was quantified in treated buffer with and without cysteine using a xylenol orange based assay (Pierce™ Quantitative Peroxide Assay Kit, Thermo Scientific, Rockford, USA). This dye was detected photometrically at 595 nm.

2.4. Ion chromatography

Nitrite (NO_2^-) and nitrate (NO_3^-) ions were detected through ion chromatography (ICS-5000, Dionex Corp., Sunnyvale, USA) in treated phosphate buffer or 2 mM cysteine in phosphate buffer. Before injection (10 µL), all the treated solution were independently diluted threefold by adding ultrapure water (MilliQ, Milli-Q® Merck KGaA, Darmstadt, Germany). An IonPac® AS23 pre-column (2 × 50 mm, Thermo Fisher Scientic Inc., Waltham, USA) coupled to an IonPac® AS23 anion exchange column (2 × 250 mm, Thermo Fisher Scientic Inc., Waltham, USA) was used for separation in an isocratic mobile phase (4.5 mM Na_2CO_3/0.8 mM $NaHCO_3$) regime and 250 µL min^{-1} flow rate. The analytes were detected by conductivity and UV detection (210 nm). The instrument was daily calibrated with the Dionex 7-anions standard.

2.5. Cysteine derivatives characterization using high-resolution mass spectrometry

Cysteine derivatives were analyzed by direct injection into a high-resolution mass spectrometer (TripleTOF5600, Sciex Ltd., Darmstadt,

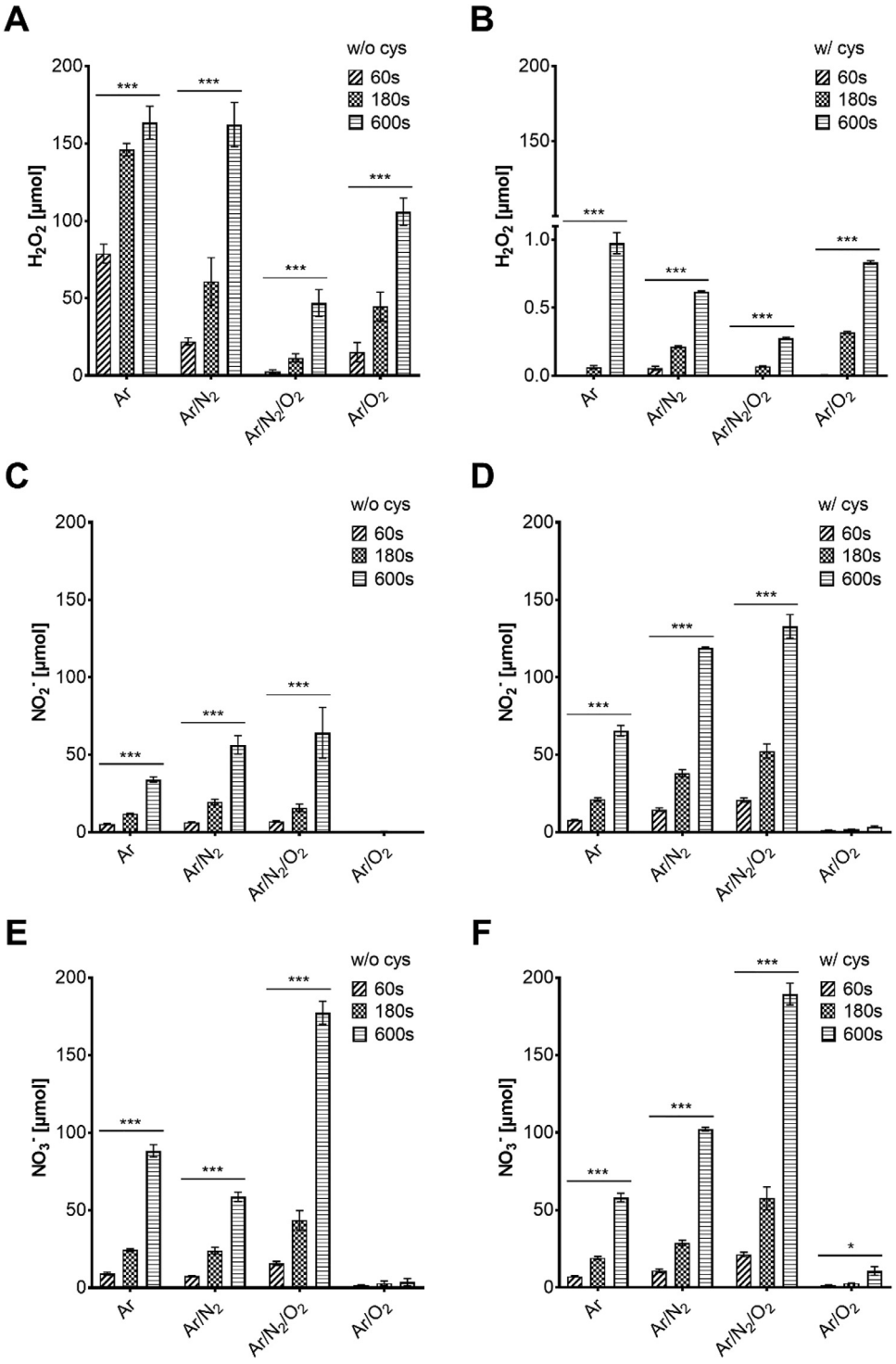

Fig. 2. Deposition of H_2O_2 (A), NO_2^- (C) and NO_3^- (E) in water or water with 2 mM cysteine (corresponding subfigures B, D, F) (kINPen09, 3 slm Ar + 1% molecular gas admix).

Germany). Each sample was diluted 1:1 with 0.3% ammonium hydroxide in methanol (negative mode) or 0.1% formic acid in methanol (positive mode) before injection. 10 µL•min^{-1} were infused by a syringe pump into an electrospray ion source running on ± 4 kV (Turbo Spray V, Sciex Ltd., Darmstadt, Germany). The following parameters were used: capillary temperature 150 °C, curtain gas: 35 slm, ion source gas 1: 20 slm, and ion source gas 2: 25 slm. MS spectra were acquired in a mass range from 50 to 400 m/z (cycle time 275 ms, accumulation time 250 ms). MS/MS spectra for each peak were acquired in order to identify the compounds (collision energy ± 24 eV, declustering potential ± 10 kV). Mass calibration was made before acquisition by using the exact mass of the most abundant compounds (e.g. cysteine, cystine). For peak identification, a minimum threshold of 300 counts s^{-1} was set, and normalized areas% were extracted for further analysis.

Table 2
Common cysteine derivatives identified after the different plasma treatments (structures in Fig. 5).

	IUPAC name (systematic name)	Traditional name	Formula	Mass [M-H]$^-$
1	2-amino-3-sulfanylpropanoic acid	Cysteine	$C_3H_7NO_2S$	120.0119
2	2,3-didehydrocysteinulic acid		$C_3H_4NO_4S$	149.986
3	cysteine 3-sulfoprop-2,3-enoic acid		$C_3H_4O_5S$	150.9701
4	2-amino-3-sulfinopropanoic acid	Cysteine sulfinic acid	$C_3H_7NO_4S$	152.0017
5	(2E)-3-sulfoprop-2-enoic acid		$C_3H_5NO_5S$	165.981
6	2-amino-3-sulfopropanoic acid	Cysteine sulfonic acid	$C_3H_7NO_5S$	167.9967
7	2-amino-3-hydroxy-3-sulfopropanoic acid		$C_3H_7NO_6S$	183.9916
8	2-amino-3-(sulfosulfanyl)propan acid	Cysteine-S-sulfonate	$C_3H_7NO_5S_2$	199.9687
9	2-amino-3-[(2-amino-2-carboxyethyl)disulfanyl]propanoic acid	Cystine	$C_6H_{12}N_2O_4S_2$	239.016
10	sulfonylideneoxidane 2-amino-2-carboxyethane-1-sulfonate)		$C_3H_9NO_9S_2$	265.9635
11	(2Z)-2-amino-3-[(2-amino-2-carboxyethanesulfinyl)sulfinyl]prop-2-enoic acid		$C_6H_{10}N_2O_6S_2$	268.9902
12	2-amino-3-[(2-amino-2-carboxyethanesulfinyl)sulfinyl]propanoic acid		$C_6H_{12}N_2O_6S_2$	271.0056
13	2-amino-3-[(2-amino-2-carboxyethanesulfonyl)sulfonyl]propanoic acid		$C_6H_{15}N_2O_8S_2$	302.9905
14	2,3-diamino-3-[(2-amino-2-carboxyethanesulfonyl)sulfonyl]propanoic acid		$C_6H_{13}N_3O_8S_2$	318.0063
15	2-amino-3-[(2-amino-2-carboxyethanesulfonyl)sulfonyl]-3-hydroxypropanoic acid		$C_6H_{12}N_2O_9S_2$	318.9899
16	2-amino-3-([2-amino-1-[(2-amino-2-carboxyethanesulfonyl)sulfonyl]-2-carboxyethyl]sulfanyl)propanoic acid		$C_9H_{16}N_3O_8S_3$	390.0100

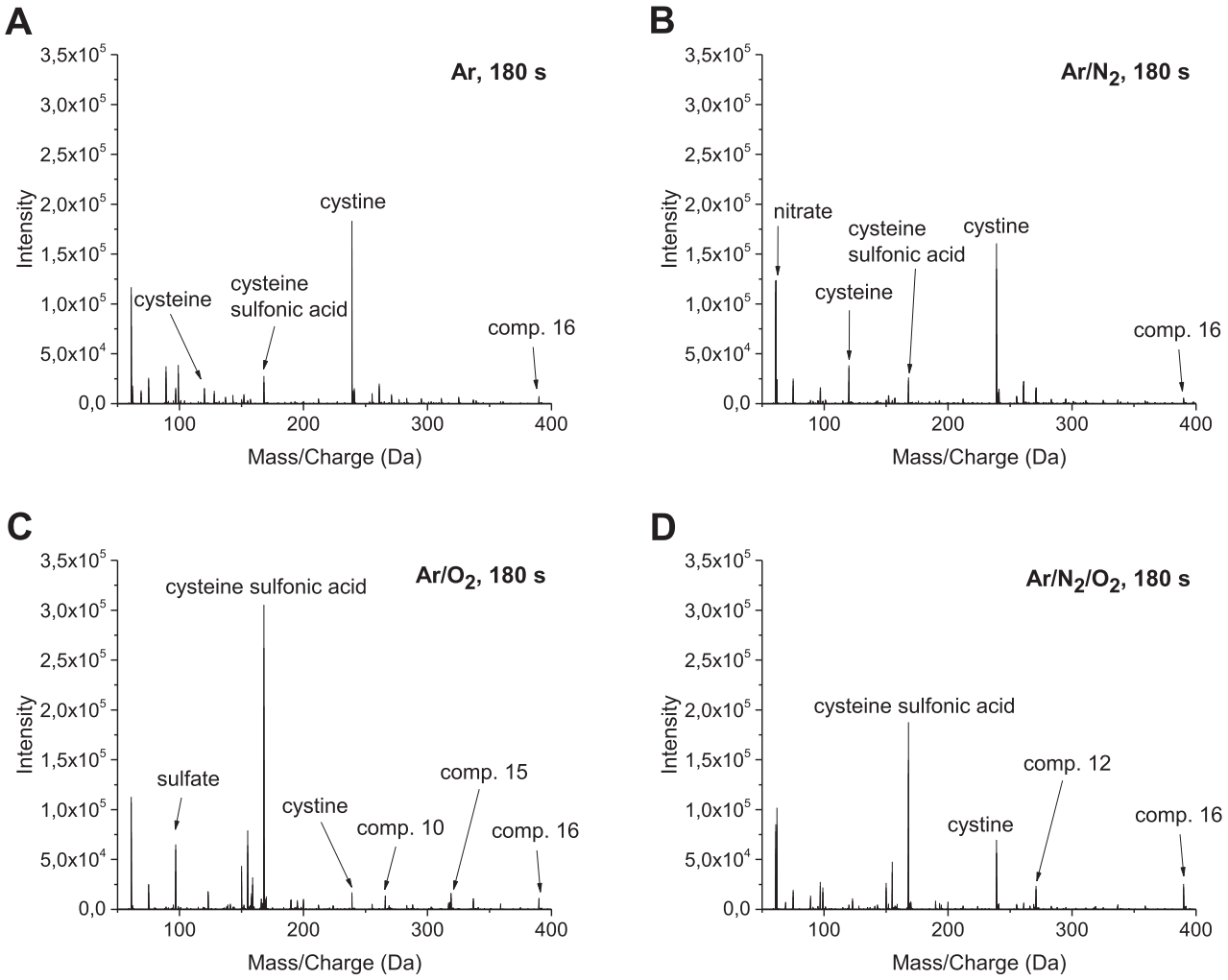

Fig. 3. High-resolution mass spectrometry traces between 50 and 400 m/z of 300 µM CAP treated cysteine (negative mode) after treatment of cysteine 300 µM by using feed gases without oxygen (Ar, Ar/N_2) (A, B), and with oxygen (Ar/O_2, Ar/N_2/O_2) (C, D) (kINPen09, 3 slm Ar + 1% molecular gas admix).

2.6. Calculation of species numbers and liquid volume in contact to gas phase

To calculate absolute numbers of cysteine molecules at the given concentration (2, 10, 100 mM) and volume (750 µl) the *Avogadro constant* (6.02×10^{23} mol^{-1}) was used, yielding 9×10^{17}, 4.5×10^{18}, and 4.5×10^{19} molecules to be treated. The number of species impinging on the treated surface was calculated using the data published by Schmidt-Bleker: a gas phase velocity of 25 m s^{-1} and a comoving volume element of 1 mm diameter describe the effluent [17]. Gas phase densities at treatment distance of 9 mm were calculated to be in the range of 10^{15} cm^{-3} for atomic O, 10^{14} cm^{-3} for $^1O_2$ and ozone (O_3),

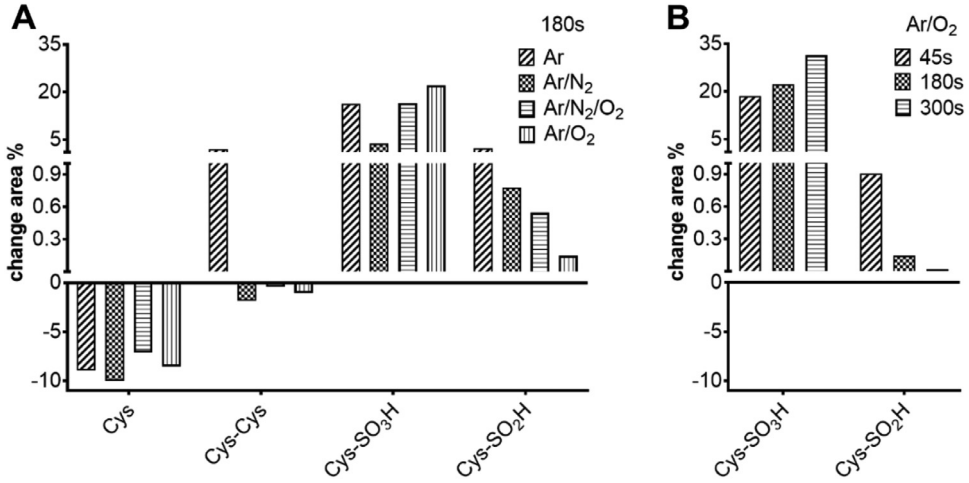

Fig. 4. Relative quantities of prominent cysteine (Cys) derivatives produced by using different feed gases (A) and treatment times (B), with focus on cystine (Cys-Cys), cysteine sulfonic acid (Cys-SO_3H) and cysteine sulfinic acid (Cys-SO_2H) (kINPen09, 3 slm Ar + 1% molecular gas admix).

and 4.5×10^{13} cm^{-3} for OH radicals [17]. To calculate the overall oxidation capacity of the mixture, the following one-electron acceptor equivalents were used: hydroxyl radical = 1, atomic O = 2, singlet oxygen = 4, ozone = 6. Superoxide anion radical was not taken into account for its reported low reactivity with cysteine. The number of cysteine molecules in the gas – liquid interface (boundary layer) was calculated using a liquid velocity of 1 m s^{-1} according to a 2-D fluid model [35] and presuming an inverted half globe shape of the liquid due to gas flow pressure (15 mm diameter). The resulting exchange of the superficial layer was estimated to take place 85 times per second. Assuming a thickness of the boundary layer of 1 µm, the volume of the surface layer in contact with the gas phase species during one second of treatment is roughly 30 mm^3 in case of the 2-D fluid model. In contrast, van Rens et al. measured a flow of 12 mm s^{-1}, also using the kINPen [36], which would correspond to a volume of 0.36 mm^3 in contact with gas phase species.

2.7. Statistical analysis and software

Three independent experiments were carried out at least in duplicates. Statistical analysis was done with two-way-ANOVA using GraphPad Prism 7. *P* values under 0.05 were considered significant. The MarvinSketch© software (version 18.8.0) was used to identify the name, the exact molecular weight, the formula and the pKa of each compound, as well as to predict the percentual amount of thiolate forms of cysteine in different pH conditions.

3. Results and discussions

3.1. Bulk oxidation of thiol groups significantly varies with feed gas composition

The oxidation of cysteine at different concentrations with various feed gas compositions (Ar, Ar/N_2, Ar/O_2, $Ar/N_2/O_2$) and treatment duration was monitored by measuring the residual free thiols after plasma treatment via Ellman´s assay (Fig. 1, Fig. 1D). Thiol group oxidation correlated with treatment time, and for 600 s all (most) free thiol groups were consumed for 2 mM (10 mM) cysteine. In contrast, only a minor increase of thiol oxidation was achieved when increasing the concentration to 100 mM (Fig. 1B/C). Further, a strong impact of feed gas composition was observed: O_2 admixture led to a significantly higher impact than argon only or nitrogen admix, which is specifically obvious with the 100 mM solution (Fig. 1C).

This indicates that reactive oxygen species generated in the gas phase from molecular oxygen, e.g. atomic O, singlet oxygen $^1O_2$, ozone or superoxide anion radicals are significant chemical partners in this model [9,17,37]. For lower concentrations (2 mM, 10 mM), cysteine conversion tends to meet a maximum which indicates saturation effects (Fig. 1A/B). From these observations, it can be concluded that long treatments and with oxygen admix in the feed gas can be considered "strongly" oxidative (Ar/O_2, $Ar/N_2/O_2$ – 300 s to 600 s), while shorter treatments, especially without oxygen in the feed gas, can be defined as "mildly" oxidative (Ar, Ar/N_2 – 60 s to 180 s). The cysteine thiol consumption efficacy is dependent on its initial concentration indicating saturation mechanisms: considering treatments of 60 s with Ar/O_2 feed gas, indeed, are oxidized around 0.75 mM of 2 mM solutions (Fig. 1A), around 3.4 mM in case of 10 mM solutions (Fig. 1B), and 4 mM in 100 mM cysteine solutions (Fig. 1C).

With that, thiol group consumption seems to be following a first-order kinetics at lower concentrations but decreases dramatically at higher concentrations (100 mM). Assumingly, the number of ROS seems to be too low in this situation. To achieve the observed oxidation, an effective flux of reactive species between 5.6×10^{15} s^{-1} and 3×10^{16} s^{-1} is necessary (table 1) and assuming a stoichiometry of 1:1 (one-electron equivalents, e.g. hydroxyl radicals) and cystine as final product (oxidation number of sulfur = −1). With cysteine sulfonic acid (oxidation number +4) as the final reaction product, a five times higher number of one-electron acceptor equivalents would be necessary (table 1). This range is in good agreement to simulations made by Schmidt-Bleker et al. [17]. At a gas phase velocity of 25 m s^{-1} and a comoving volume element of 1 mm diameter a number of 2×10^{16} s^{-1} oxygen atoms, each 2×10^{15} s^{-1} $^1O_2$ and O_3 molecules, and 9×10^{14} s^{-1} OH radicals hit the liquid target. Taken together and weighed by their electron acceptor equivalents this corresponds to 6.1×10^{16} one-electron acceptor equivalents per second (table 1). While this amount is sufficient to oxidize the 2 mM cysteine solution in full, the number is too low in case of the 10 mM, and even more so the 100 mM solution. For both, the estimated number of electron acceptor equivalents matches about twice the number of equivalents necessary to transform cysteine into cystine. Subsequently, predominantly cysteine was observed for the 100 mM solution with very limited amounts of higher oxidized cysteine derivatives, showing the plausibility of these estimates.

For the 10 mM solution, a mixed behavior was observed: although the ratio of overall number of cysteine molecules being oxidized and number of electron acceptor equivalents deposited per second is 1:2. Hence, only limited further oxidation is possible and the theoretical final product would be cysteine sulfenic acid, which was not observed. Instead, a significant amount of higher oxidized derivatives was found, pointing at substrate limitation processes at the gas – liquid interface.

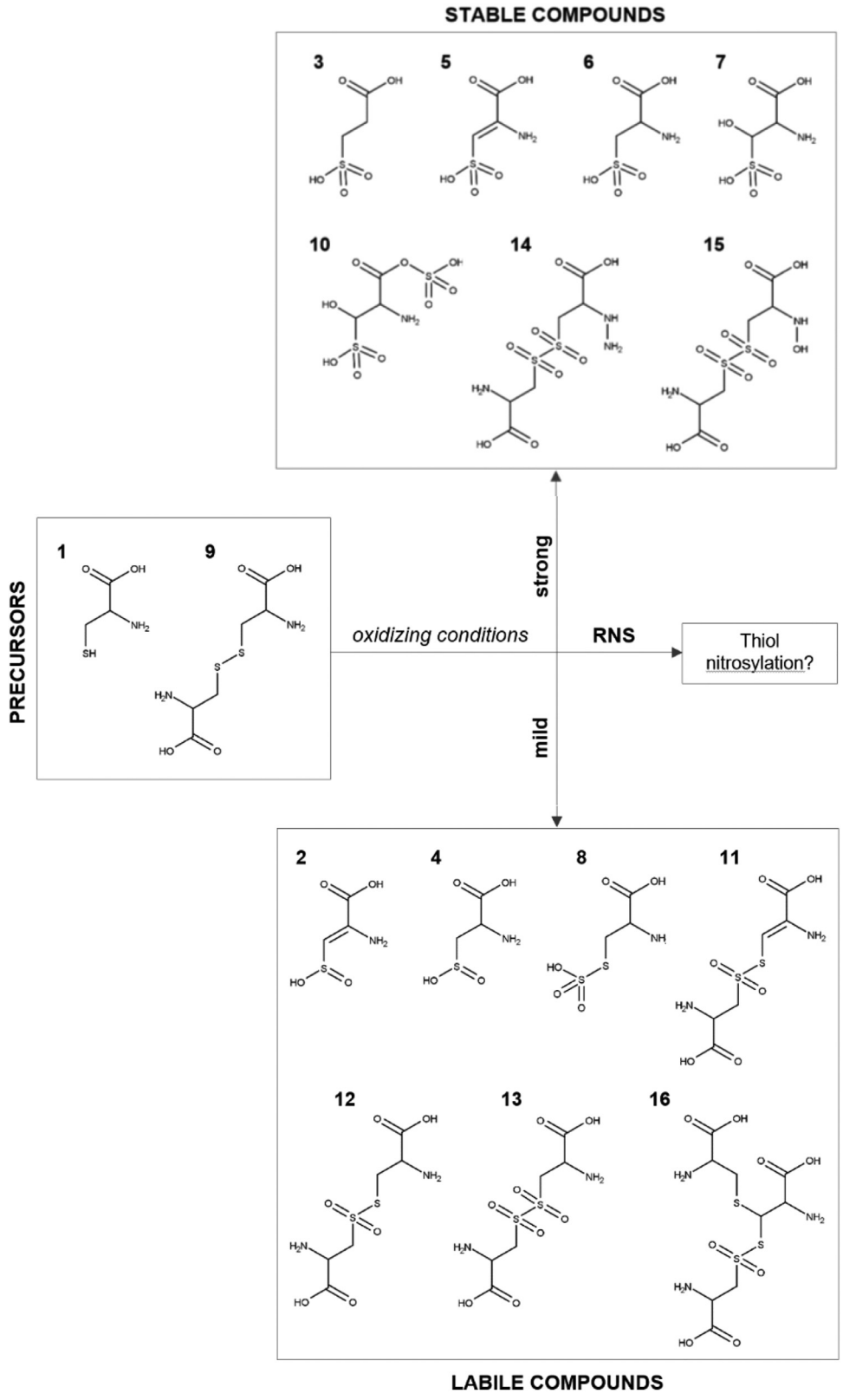

Fig. 5. Cysteine and cystine (compounds 1 and 9, shown as precursors here) derivatives categorization in labile and stable compounds in relation to their optimal conditions of production, which can be mild (Ar, Ar/N_2 – 60 s to 180 s) or strong (Ar/O_2, $Ar/N_2/O_2$ – 300 s to 600 s) conditions.

Atomic oxygen or hydroxyl radicals will react at the interfacial layer at very fast rates in the order of 10^{-9} M^{-1} s^{-1}. Thus, the consumption of target molecules might be faster than bulk liquid transport (convection), resulting in the depletion of cysteine in the surface layer and enrichment of reaction products which may be attacked further. When assuming a liquid phase velocity of 1 m s^{-1} or 12 mm s^{-1}, a half globe shape of the liquid due to gas flow, and a boundary (interface) layer of 1 μm thickness (see 2.6), the volume of the surface layer treated

during one second is roughly 30 mm^3 (2-D model) or 0.36 mm^3 (measurement). Consequently, an estimation of cysteine molecules exposed to the plasma-generated species at the boundary layer can be made, ranging between 6.3×10^{14} and 1.8×10^{18} (see table 1). Using the 2D-model assumption, the number of potentially exposed cysteine molecules in the boundary layer is 10 – 50 fold higher than oxidized in the experiment. In contrast, assuming the 12 mm s^{-1} velocity of the liquid, the observed number of oxidized cysteine molecules is 10 fold higher than the number of molecules present at the boundary in the 2 mM and 10 mM solutions, while model and observation correlate reasonably in the 100 mM case. Taken together, this seems to suggest that the 2D-model is wrong and the measured 80fold slower flow rate of the liquid correct. On the other hand, when considering a slow reaction rate of some species deposited in the liquid, e.g. the superoxide anion radical, a limited number of cysteine molecules can be attacked efficiently and the 2D-model correct. This disparity might further be augmented by various factors, like wrong assumptions regarding the boundary layer thickness and indicates that further research is necessary to explain these results in full.

In part, the aberration between assumption and measurement can be explained by pH effects, with high cysteine concentration leading to a slightly lower pH (10 mM, pH 6.02; 100 mM, pH 5.85) than lower concentrations (2 mM, pH 6.53). Due to the pKa of the thiol group (pKa ≈ 10.2), the percentage of thiolates decrease with decreasing pH. Using the MarvinSketch© software, the equilibrium concentration of cysteine thiolate can be calculated to be 1.6 μM (2 mM solutions), 2 μM (10 mM solutions), and 10 μM (100 mM solutions). Considering the thiolate being more reactive than the thiol, the impact of long-lived hydrogen peroxide species would be emphasized. The data illustrate the necessity to observe or control pH during plasma treatment of biological materials as local conditions can vary drastically, e.g. between normal skin (pH 5.5), saliva (pH 7.4), or chronic wounds (pH 7.2 – 8.9) [40].

To obtain a general idea of the deposition of long lives species under the treatment conditions in the presence or absence of cysteine (2 mM), hydrogen peroxide (H_2O_2), nitrite (NO_2^-), and nitrate (NO_3^-) were quantified (Fig. 2). For all three species, it can be concluded that the deposition increases with treatment duration, regardless of working gas composition, marking them as “stable” species [18, 24]. As H_2O_2 is the final product of many ROS, nitrate ions are the end product accumulating from unstable reactive nitrogen species, such as peroxynitrite ($ONOO^-$) and nitric oxide radicals (•NO).

High amounts of hydrogen peroxide are reached by treatments with Ar and Ar/N_2 feed gas compositions (up to 170 μM, Fig. 2A). When oxygen is in the feed gas admix, a maximum of 100 μM was detected. H_2O_2 derives from the recombination of OH radicals, that can be created in the gas phase from water vapor [41,42] or in the liquid phase, e.g. by photolysis of water [43] or electron impact. The contribution of the latter two might be significant, as a dry nitrogen gas curtain is used to reduce the lateral diffusion of ambient species into the effluent and limiting the formation of gas phase OH radicals. The second source of H_2O_2 is the disproportionation of OOH radicals, which is favored in slightly acidic conditions (see above). The contribution of this pathway seems to be minor, as O_2^- radicals are produced especially if molecular oxygen is present. However, under these conditions lowest H_2O_2 amounts were observed. The deposition of H_2O_2 is significantly reduced when cysteine is present (≤ 1 μM, Fig. 2B), indicating its consumption and/or reduced formation. RNS deposition (Fig. 2C/E), occurs predominantly in N_2/O_2 or N_2 admix when compared to Ar only treatment. For Ar/O_2, only negligible amounts of nitrite/nitrate were measured. In the presence of cysteine, nitrite deposition is generally higher than in its absence, with traces even with Ar/O_2 detected while highest values were achieved for N_2/O_2 admix (Fig. 2D). Nitrate deposition (Fig. 2F) was unaffected by the presence of cysteine as a reaction partner, indicating its origin from gas phase derived precursors with little reaction probability (e.g. HNO_3, N_2O_5). The nitrate ion itself is stable under the conditions present. In general, the presence of a potential reaction partner modulates the observable deposition of long-lived species, a fact also observed by Privat-Maldonado [44]. While scavenging away the precursors of H_2O_2 formation (OH radicals, O_2^-/OOH radicals) or reacting with itself (thiolate ions, forming cystine) [28, 45], nitrite deposition is favored. As RNS chemistry is not well understood, several possibilities for explanation exist: reactive nitrogen species such as N_2O_3 or $ONOO^-$ attack the cysteine and nitrite ions are byproducts, NO_2 radicals are not converted to NO but nitrite due to the lack of atomic oxygen [46], or – less likely – nitrite is oxidized to nitrate in a lesser extent. However, this latter option would require nitrate deposition to increase, which was not observed. Although closely related, this is a further indication that nitrite and nitrate are produced by different pathways and that nitrate does not originate from nitrite. Clearly, active RNS species and their trajectories need further attention.

3.2. CAP-derived reactive species generate a rich variety of cysteine derivatives

As has been suggested by Zhou and Takai that amino acids are targets for plasma-derived species [26,47]. In similar approaches, both looked into the oxidation of cysteine by CAP and found its dimer cystine and cysteine sulfonic acid. These major products have also been identified in the current approach along with around 20 further cysteine derivatives of different oxidation state and molecular structure, expanding the knowledge of the previous works. Cystine (m/z = 239.016) was identified as the dominant compound in Ar or Ar/N_2 plasma treatments and cysteine sulfonic acid (m/z = 167.9967) dominant in O_2 admix plasma treatments (Ar/O_2, Ar/N_2/O_2). Potentially bioactive cystine derivatives are generated predominantly with O_2 or N_2/O_2 admixtures with masses > 250 Da. Further prominent cysteine/cystine products detected and structurally resolved are shown in Table 2 and Fig. 5.

Clearly, an oxygen species driven oxidation of the thiol moiety is the most abundant modification, with some derivatives being biologically relevant (reactive sulfur species, RSS).

One of the key roles in the redox signaling is presumably assigned to cysteine sulfenic acid (m/z = 136.0068) that was not detected due to its instability. It is rapidly oxidized to cysteine sulfenic acid (Cys-SO_2H, compound 2) and to cysteine sulfonic acid (Cys-SO_3H, compound 3) [29,48], which may be a final product of plasma treatment. Cysteine sulfenic acid may react with itself, producing oxidized forms of cystine such as di-sulfoxides (m/z = 268.9902, compound 11; m/z = 271.0056, compound 12). Under the further impact of oxidative species, cysteine sulfonic acid appears as “apex” product.

Cystine (resp. its disulfide bridge as a structural element) is essential for protein structure, function, interactions, and subcellular localization [49]; indeed, the cysteine-cystine system is one of the most sensitive sensors of the redox state of a cell, both its physiological and pathological state [48,50]. Highly oxidized variants of cystine, such as di-sulfoxides or tetra-sulfoxides (m/z = 302.9905, compound 13; m/z = 318.0063, compound 14; m/z = 318.9899, compound 15), occur and have been shown to have an anti-proliferative effect on cancer cells [32,33,51]. Another bioactive derivative is the *S*-nitrosocysteine (m/z = 149.0021), which is one of the most important post-translational protein modifications. It is considered essential in cardiac functioning, cancer biology, and wound healing for its role in the nitric oxide pathway [52–55].

The production of *S*-nitrosocysteine was not observed albeit it was predicted by simulations [28]. Various reasons could lead to this discrepancy: (a) the reactive nitrogen species are not as effective as predicted; b) the products decay easily; c) RNS facilitate oxidation, but do not form covalent bonds between C or S and N. The first option seems least consistent, since in Ar/N_2 conditions the oxidation of cysteine is considerably high (Fig. 1). However, significant deposition of the ROS H_2O_2 also occurs. Further studies focusing on the role of plasma-derived RNS on biomolecules are desirable.

3.3. Cysteine derivatives profiles reflect the treatment conditions and the ROS production

As indicated in Fig. 3, the generation of cysteine derivatives was dependent on the conditions used, with each parameter set producing a different product profile, either qualitatively or quantitatively (Fig. 3/4). In strongly oxidizing conditions (e.g. presence of oxygen in the feed gas) products showing a strong oxidation of the cysteine thiol group are observed (Fig. 4A); this is in accordance with the analysis of residual free thiols measured after the same treatment via colorimetric assay by using the Ellman's reagent (Fig. 1). In milder conditions, cystine (Cys-Cys) and cysteine sulfinic acid (Cys-SO_2H) can be detected after the treatment (e.g. Ar only), but in presence of molecular gases further oxidations of these occur, predominantly with O_2 admixtures, leading to their destruction (Fig. 4A). In contrast, cysteine sulfonic acid (Cys-SO_3H) accumulated, even with oxygen in the feed gas (Fig. 4B).

Besides the direct oxidation of cysteine, also the oxidation of cystine and its oxidized disulfides can lead to this product. It is the most abundant compound produced, even when the final products in the applied treatment regimen are inorganic sulfate and the amino acid alanine.

In general, cysteine sulfonic acid and cysteine sulfinic acid are compounds that are archetypical for the behavior of most other cysteine derivatives identified. Indeed, they could be divided into two groups: a) stable compounds, which increase in long and often oxygen-dominated treatments (Ar/O_2, $Ar/N_2/O_2$), b) labile compounds, which decrease in strong conditions but are present after short treatments predominantly without oxygen in the feed gas (Ar, Ar/N2).

All identified cysteine derivatives are shown in Fig. 5 are classified on the base of these two groups. It can be stated that all compounds can be generated from cystine too, as the disulfide moiety can be easily attacked by plasma generated species except hydrogen peroxide which was ineffective (data not shown).

With that, the produced cysteine derivatives profiles represent the treatment conditions, reflecting the chemical foodprint of cold plasma in liquids when discharge parameters are modulated. The reactive species predominantly deposited by the discharge in the aqueous system determined the product portfolio with the short-lived species, atomic oxygen (O), singlet oxygen ($^1O_2$), hydroxyl radicals (OH), and superoxide anion radicals (O_2^-) being major players. The responsible short-lived species have so far not been pinpointed, but further investigations are underway. Hydrogen peroxide, which is deposited in large amounts under some conditions, reacts with the thiolate form of cysteine only and leads to the formation of cystine via cysteine sulfenic acid [28,56]. Indeed, the highest amount of deposited hydrogen peroxide was measured for argon feed gas (Fig. 4A), along with the highest amount of cystine (Fig. 2). This shows that H_2O_2 has a limited impact on the observed compound portfolio. The long-lived ROS ozone may be a candidate to be responsible for some of the products; however, its deposition in liquids remains debatable due to its solubility. Data suggest a potential for ozone to contribute to higher oxidized products, such as cysteine sulfonic acid (compound 3) or oxidized cystine derivatives, e. g. tetra-sulfoxides (compounds 14 and 15) [57].

Ultimately, the physiological impact of the plasma-derived species on biomolecule resident thiols needs to be shown. Already, the oxidation of the redox sensor protein NRF2-thiol groups was shown to be triggered by plasma treatment and led to changes in anti-oxidant protein transcription [58]. So far, it remains to be clarified if this oxidation was executed by plasma-derived species or secondary species deriving from oxidized lipid membranes or leaky mitochondria. In regard to the short free diffusion ranges of most plasma-derived species, it must be presumed that direct interaction with intracellular proteins is not likely. However, oxidation of membrane-bound proteins, such as structural proteins for cell-cell and cell-matrix contact, pore proteins, and receptors might be targeted directly. Further, bioactive derivatives of small molecules, like the here delineated CAP derived cysteine products, may contribute. First experiments using oxidized cysteine solutions showed changes in mammalian cell migration and metabolism (Heusler et al., same special issue).

4. Summary and conclusion

The plasma liquid chemistry produced by an argon plasma jet (kINPen) has been investigated via cysteine as a model substance. The intensity of cysteine oxidation increased with treatment duration and presence of oxygen admixture in the feed gas, while it decreased with higher cysteine concentration in the liquid. The number of thiol groups consumed per second of discharge were two to ten-fold lower than the number of plasma-derived one-electron acceptor equivalents hitting the surface during this time. Taking into account the number of cysteine molecules in the boundary layer and the achieved oxidation state, it can be stated that short-lived species react at the interface with the target and only limited conversion takes place in the bulk. Especially the long-lived hydrogen peroxide was found ineffective in yielding oxidized cysteine derivatives. When comparing turnover rates for low and high concentration of tracer boundary layer depletion was observed, an indicator for short-lived ROS like atomic O or singlet oxygen. Still, as model and measurement do not correlate ideally, further research is needed to clarify the role of the interface in cysteine derivatization. A range of products from cysteine was identified, in part indicative for certain treatment conditions. Several non-stable products occur transiently during the plasma treatment. Bioactive reactive sulfur species (RSS) have been found for mild treatment conditions, such as cysteine sulfoxides and cysteine-*S*-sulfonate, allowing secondary effects being triggered via their cellular recognition. When translating these observations into the in-vivo application, strong direct oxidation of protein thiol groups with subsequent changes in protein biochemistry must be considered.

Acknowledgments

Funding from the German Federal Ministry of Education and Research(grant number 03Z22DN12 to K.W.) supported this work. The experimental contribution of Johann Volzke and Dana Sponholz is gratefully acknowledged.

Conflict of interest

The authors declare no conflict of interest.

Supplementary materials

Supplementary material associated with this article can be found, in the online version, at doi:10.1016/j.cpme.2019.100083.

References

[1] K.D. Weltmann, T. von Woedtke, Plasma medicine-current state of research and medical application, Plasma Phys. Control. Fusion 59 (1) (2017) 014031.
[2] C. Ulrich, F. Kluschke, A. Patzelt, S. Vandersee, V.A. Czaika, H. Richter, A. Bob, J. von Hutten, C. Painsi, R. Hugel, A. Kramer, O. Assadian, J. Lademann, B. Lange-Asschenfeldt, Clinical use of cold atmospheric pressure argon plasma in chronic leg ulcers: A pilot study, J. Wound Care 24 (5) (2015) 196–203.
[3] S. Emmert, F. Brehmer, H. Hänßle, A. Helmke, N. Mertens, R. Ahmed, D. Simon, D. Wandke, W. Maus-Friedrichs, G. Däschlein, M.P. Schön, W. Viöl, Atmospheric pressure plasma in dermatology: Ulcus treatment and much more, Clin. Plas. Med. 1 (1) (2013) 24–29.
[4] S. Bekeschus, A. Schmidt, K.-D. Weltmann, T. von Woedtke, The plasma jet kINPen—A powerful tool for wound healing, Clin. Plas. Med. 4 (1) (2016) 19–28.
[5] P.J. Bruggeman, M.J. Kushner, B.R. Locke, J.G.E. Gardeniers, W.G. Graham, D.B. Graves, R.C.H.M. Hofman-Caris, D. Maric, J.P. Reid, E. Ceriani, D.F. Rivas, J.E. Foster, S.C. Garrick, Y. Gorbanev, S. Hamaguchi, F. Iza, H. Jablonowski, E. Klimova, J. Kolb, F. Krcma, P. Lukes, Z. Machala, I. Marinov, D. Mariotti, S.M. Thagard, D. Minakata, E.C. Neyts, J. Pawlat, Z.L. Petrovic, R. Pflieger, S. Reuter, D.C. Schram, S. Schroter, M. Shiraiwa, B. Tarabova, P.A. Tsai, J.R.R. Verlet, T. von Woedtke, K.R. Wilson, K. Yasui, G. Zvereva, Plasma-liquid

interactions: A review and roadmap, Plasma Sources Sci. T 25 (5) (2016) 053002.
[6] T. von Woedtke, H.R. Metelmann, K.D. Weltmann, Clinical Plasma Medicine, State and perspectives of in vivo application of cold atmospheric plasma, Contrib. Plasma Phys. 54 (2) (2014) 104–117.
[7] D.B. Graves, Mechanisms of plasma medicine: Coupling plasma physics, Biochem. Biol. 1 (4) (2017) 281–292.
[8] A. Schmidt-Bleker, S. Reuter, K.D. Weltmann, Quantitative schlieren diagnostics for the determination of ambient species density, gas temperature and calorimetric power of cold atmospheric plasma jets, J. Phys. D Appl. Phys 48 (17) (2015) 175202.
[9] S. Reuter, H. Tresp, K. Wende, M.U. Hammer, J. Winter, K. Masur, A. Schmidt-Bleker, K.D. Weltmann, From RONS to ROS: tailoring Plasma Jet Treatment of Skin Cells, IEEE Trans. Plasma Sci. 40 (11) (2012) 2986–2993.
[10] A. Schmidt-Bleker, S. Reuter, K.-D. Weltmann, Non-dispersive path mapping approximation for the analysis of ambient species diffusion in laminar jets, Phys. Fluids (1994–present) 26 (8) (2014) 083603.
[11] B. Van Ham, S. Hofmann, R. Brandenburg, P. Bruggeman, In situ absolute air, O3 and NO densities in the effluent of a cold RF argon atmospheric pressure plasma jet obtained by molecular beam mass spectrometry, J. Phys. D Appl. Phys. 47 (22) (2014) 224013.
[12] S. Iseni, S. Zhang, A.F.H. van Gessel, S. Hofmann, B.J.T. van Ham, S. Reuter, K.D. Weltmann, P.J. Bruggeman, Nitric oxide density distributions in the effluent of an RF argon APPJ: Effect of gas flow rate and substrate, New J. Phys. 16 (12) (2014) 123011.
[13] S. Zhang, W. van Gaens, B. van Gessel, S. Hofmann, E. van Veldhuizen, A. Bogaerts, P. Bruggeman, Spatially resolved ozone densities and gas temperatures in a time modulated RF driven atmospheric pressure plasma jet: An analysis of the production and destruction mechanisms, J. Phys. D Appl. Phys. 46 (20) (2013) 205202.
[14] J. Golda, J. Held, B. Redeker, M. Konkowski, P. Beijer, A. Sobota, G. Kroesen, N.S.J. Braithwaite, S. Reuter, M.M. Turner, T. Gans, D. O'Connell, V. Schulz-von der Gathen, Concepts and characteristics of the 'COST reference microplasma jet', J. Phys. D Appl. Phys. 49 (8) (2016) 084003.
[15] S. Schneider, J.W. Lackmann, F. Narberhaus, J.E. Bandow, B. Denis, J. Benedikt, Separation of VUV/UV photons and reactive particles in the effluent of a He/O2atmospheric pressure plasma jet, J. Phys. D Appl. Phys. 44 (29) (2011) 295201.
[16] Y. Gorbanev, C.C.W. Verlackt, S. Tinck, E. Tuenter, K. Foubert, P. Cos, A. Bogaerts, Combining experimental and modelling approaches to study the sources of reactive species induced in water by the COST RF plasma jet, Phys. Chem. Chem. Phys 20 (4) (2018) 2797–2808.
[17] A. Schmidt-Bleker, J. Winter, A. Bösel, S. Reuter, K.-D. Weltmann, On the plasma chemistry of a cold atmospheric argon plasma jet with shielding gas device, Plasma Sources Sci. Technol. 25 (1) (2015) 015005.
[18] H. Tresp, M.U. Hammer, K.-D. Weltmann, S. Reuter, Effects of atmosphere composition and liquid type on plasma-generated reactive species in biologically relevant solutions, Plasma Med. 3 (1–2) (2013) 45–55.
[19] H. Jablonowski, M.A.C. Hänsch, M. Dünnbier, K. Wende, M.U. Hammer, K.-D. Weltmann, S. Reuter, T. von Woedtke, Plasma jet's shielding gas impact on bacterial inactivation, Biointerphases 10 (2) (2015) 029506.
[20] K. Wende, P. Williams, J. Dalluge, W. Van Gaens, H. Aboubakr, J. Bischof, T. von Woedtke, S.M. Goyal, K.-D. Weltmann, A. Bogaerts, P. Bruggeman, Identification of the biologically active liquid chemistry induced by a nonthermal atmospheric pressure plasma jet, Biointerphases 10 (2) (2015) 029518.
[21] H. Jablonowski, J.S. Sousa, K.-D. Weltmann, K. Wende, S.J.S.r. Reuter, Quantification of the ozone and singlet delta oxygen produced in gas and liquid phases by a non-thermal atmospheric plasma with relevance for medical treatment, 8(1) (2018) 12195.
[22] Y. Gorbanev, N. Stehling, D. O'Connell, V. Chechik, Reactions of nitroxide radicals in aqueous solutions exposed to non-thermal plasma: Limitations of spin trapping of the plasma induced species, Plasma Sources Sci. Technol. 25 (5) (2016) 055017.
[23] H. Jablonowski, T. von Woedtke, Research on plasma medicine-relevant plasma–liquid interaction: What happened in the past five years? Clin. Plas. Med. 3 (2) (2015) 42–52.
[24] J. Winter, H. Tresp, M.U. Hammer, S. Iseni, S. Kupsch, A. Schmidt-Bleker, K. Wende, M. Dunnbier, K. Masur, K.D. Weltmannan, S. Reuter, Tracking plasma generated H2O2 from gas into liquid phase and revealing its dominant impact on human skin cells, J. Phys. D Appl. Phys. 47 (28) (2014) 285401.
[25] A.R. Gibson, H.O. McCarthy, A.A. Ali, D. O'Connell, W.G. Graham, Interactions of a non-thermal atmospheric pressure plasma effluent with PC-3 prostate cancer cells, Plasma Process. Polym. 11 (12) (2014) 1142–1149.
[26] R. Zhou, R. Zhou, J. Zhuang, Z. Zong, X. Zhang, D. Liu, K. Bazaka, K. Ostrikov, Interaction of atmospheric-pressure air microplasmas with amino acids as fundamental processes in aqueous solution, PLoS One 11 (5) (2016) e0155584.
[27] C. Klinkhammer, C. Verlackt, D. Smilowicz, F. Kogelheide, A. Bogaerts, N. Metzler-Nolte, K. Stapelmann, M. Havenith, J.W. Lackmann, Elucidation of plasma-induced chemical modifications on glutathione and glutathione disulphide, Sci. Rep. 7 (1) (2017) 13828.
[28] J.W. Lackmann, K. Wende, C. Verlackt, J. Golda, J. Volzke, F. Kogelheide, J. Held, S. Bekeschus, A. Bogaerts, V. Schulz-von der Gathen, K. Stapelmann, Chemical fingerprints of cold physical plasmas—An experimental and computational study using cysteine as tracer compound, Sci. Rep. 8 (1) (2018) 7736.
[29] C.E. Paulsen, K.S. Carroll, Cysteine-mediated redox signaling: chemistry, biology, and tools for discovery, Chem. Rev. 113 (7) (2013) 4633–4679.
[30] D. Yan, A. Talbot, N. Nourmohammadi, X. Cheng, J. Canady, J. Sherman, M. Keidar, Principles of using cold atmospheric plasma stimulated media for cancer treatment, Sci. Rep. 5 (2015) 18339.
[31] E. Takai, T. Kitamura, J. Kuwabara, S. Ikawa, S. Yoshizawa, K. Shiraki, H. Kawasaki, R. Arakawa, K. Kitano, Chemical modification of amino acids by atmospheric-pressure cold plasma in aqueous solution, J. Phys. D Appl. Phys. 47 (28) (2014) 285403.
[32] G.I. Giles, K.M. Tasker, C. Jacob, Oxidation of biological thiols by highly reactive disulfide-S-oxides, Gen. Physiol. Biophys. 21 (1) (2002) 65–72.
[33] G.I. Giles, M.J. Nasim, W. Ali, C. Jacob, The reactive sulfur species concept: 15 years on, Antioxidants (Basel) 6 (2) (2017) 38.
[34] C. Jacob, G.I. Giles, N.M. Giles, H. Sies, Sulfur and selenium: the role of oxidation state in protein structure and function, Angew. Chem. Int. Ed. Engl. 42 (39) (2003) 4742–4758.
[35] C.C.W. Verlackt, W. Van Boxem, A. Bogaerts, Transport and accumulation of plasma generated species in aqueous solution, Phys. Chem. Chem. Phys. 20 (10) (2018) 6845–6859.
[36] J.F.M. van Rens, J.T. Schoof, F.C. Ummelen, D.C. van Vugt, P.J. Bruggeman, E.M. van Veldhuizen, Induced liquid phase flow by RF Ar cold atmospheric pressure plasma jet, IEEE T Plasma Sci. 42 (10) (2014) 2622–2623.
[37] A. Schmidt-Bleker, J. Winter, S. Iseni, M. Dunnbier, K.D. Weltmann, S. Reuter, Reactive species output of a plasma jet with a shielding gas device-combination of FTIR absorption spectroscopy and gas phase modelling, J. Phys. D: Appl. Phys. 47 (14) (2014).
[38] C.C.W. Verlackt, et al., Transport and accumulation of plasma generated species in aqueous solution, Phys. Chem. Chem. Phys. 20 (10) (2018) 6845–6859.
[39] J.F. Van Rens, J.T. Schoof, F.C. Ummelen, D.C. Van Vugt, P.J. Bruggeman, E. Van Veldhuizen, Induced liquid phase flow by RF Ar cold atmospheric pressure plasma jet, IEEE Trans. Plasma Sci. 42 (10) (2014) 2622–2623.
[40] L.M. Bennison, CN. Miller, RJ Summers, AMB Minnis, G Sussman, W McGuiness, The pH of wounds during healing and infection: A descriptive literature review, Wound Practice Res. 25 (2) (2017) 7.
[41] Y. Gorbanev, D. O'Connell, V. Chechik, Non-thermal plasma in contact with water: The origin of species, Chemistry (Easton) 22 (10) (2016) 3496–3505.
[42] W. Van Boxem, J. Van der Paal, Y. Gorbanev, S. Vanuytsel, E. Smits, S. Dewilde, A. Bogaerts, Anti-cancer capacity of plasma-treated PBS: Effect of chemical composition on cancer cell cytotoxicity, Sci. Rep. 7 (1) (2017) 16478.
[43] S. Robl, M. Worner, D. Maier, A.M. Braun, Formation of hydrogen peroxide by VUV-photolysis of water and aqueous solutions with methanol, Photochem. Photobiol. Sci 11 (6) (2012) 1041–1050.
[44] A. Privat-Maldonado, D. O'Connell, E. Welch, R. Vann, M.W. van der Woude, Spatial dependence of DNA damage in bacteria due to low-temperature plasma application as assessed at the single cell level, Sci. Rep. 6 (2016) 35646.
[45] D. Luo, S.W. Smith, B.D. Anderson, Kinetics and mechanism of the reaction of cysteine and hydrogen peroxide in aqueous solution, J. Pharm. Sci. 94 (2) (2005) 304–316.
[46] H. Jablonowski, A. Schmidt-Bleker, K.D. Weltmann, T. von Woedtke, K. Wende, Non-touching plasma-liquid interaction— Where is aqueous nitric oxide generated? Phys. Chem. Chem. Phys. 20 (39) (2018) 25387–25398.
[47] E. Takai, T. Kitamura, J. Kuwabara, S. Ikawa, S. Yoshizawa, K. Shiraki, H. Kawasaki, R. Arakawa, K. Kitano, Chemical modification of amino acids by atmospheric-pressure cold plasma in aqueous solution, J. Phys. D 47 (28) (2014) 285403.
[48] Y.-M. Go, J.D. Chandler, D.P. Jones, The cysteine proteome, Free Radic. Biol. Med. 84 (2015) 227–245.
[49] N.O. Baez, J.A. Reisz, C.M. Furdui, Mass spectrometry in studies of protein thiol chemistry and signaling: Opportunities and caveats, Free Radic. Biol. Med. 80 (2015) 191–211.
[50] L.B. Poole, The basics of thiols and cysteines in redox biology and chemistry, Free Radic. Biol. Med. 80 (2015) 148–157.
[51] J. Borlinghaus, F. Albrecht, M.C. Gruhlke, I.D. Nwachukwu, A.J. Slusarenko, Allicin: Chemistry and biological properties, Molecules 19 (8) (2014) 12591–12618.
[52] A.A. Ali, J.A. Coulter, C.H. Ogle, M.M. Migaud, D.G. Hirst, T. Robson, H.O. McCarthy, The contribution of N(2)O(3) to the cytotoxicity of the nitric oxide donor DETA/NO: An emerging role for S-nitrosylation, Biosci. Rep. 33 (2) (2013) e00031.
[53] C. Belge, P.B. Massion, M. Pelat, J.L. Balligand, Nitric oxide and the heart: Update on new paradigms, Ann. N. Y. Acad. Sci 1047 (2005) 173–182.
[54] A.C. Kendall, J.L. Whatmore, P.G. Winyard, G.R. Smerdon, P. Eggleton, Hyperbaric oxygen treatment reduces neutrophil-endothelial adhesion in chronic wound conditions through S-nitrosation, Wound Repair Regen. 21 (6) (2013) 860–868.
[55] B. Stallmeyer, H. Kampfer, N. Kolb, J. Pfeilschifter, S. Frank, The function of nitric oxide in wound repair: inhibition of inducible nitric oxide-synthase severely impairs wound reepithelialization, J. Invest. Dermatol. 113 (6) (1999) 1090–1098.
[56] Z. Abedinzadeh, M. Gardesalbert, C. Ferradini, Kinetic-study of the oxidation mechanism of glutathione by hydrogen-peroxide in neutral aqueous-medium, Can. J. Chem. Revue Canadienne De Chimie 67 (7) (1989) 1247–1255.
[57] G.N. Khairallah, A.T. Maccarone, H.T. Pham, T.M. Benton, T. Ly, G. da Silva, S.J. Blanksby, R.A. O'Hair, Radical formation in the gas-phase ozonolysis of deprotonated cysteine, Angew. Chem. Int. Ed. Engl. 54 (44) (2015) 12947–12951.
[58] A. Schmidt, S. Dietrich, A. Steuer, K.-D. Weltmann, T. von Woedtke, K. Masur, K. Wende, Non-thermal plasma activates human keratinocytes by stimulation of antioxidant and phase II pathways, J. Biol. Chem. 290 (11) (2015) 6731–6750.